METHODOLOGY FOR THE DESIGN CALCULATION OF A HYDRAULIC PULSE DRIVE CONTROLLED BY A SINGLE-STAGE HIGH-CAPACITY PRESSURE PULSE GENERATOR

Roman Obertyukh [1[0000-0003-2939-6582]], *Andrii Slabkyi* [1[0000-0001-9284-2296]], *Oleksandr Povstyanoy* [2[0000-0002-1416-225X]], *Serhiy Kotyk* [1[0009-0000-9396-7189]], *Olha Serdiuk* [1[0009-0001-0082-2990]]
[1]*Vinnytsia National Technical University, Khmelnytske highway 95, Vinnytsia 21021, Ukraine*
[2]*Lutsk National Technical University, Lvivska street, 75, Volyn region, 43018, Lutsk, Ukraine,*

Abstract - This article presents a scientifically sound methodology for the design calculation of a hydraulic pulse drive (HPD) equipped with a new type of single-stage parametric pressure pulse generator (PPG) with increased throughput. The main scientific innovation of the developed design is the integration of the sealing elements of the first and second sealing stages with a high-linearity slotted spring. This technical solution has enabled a transition from a traditional spool seal to a valve (face) seal, which minimises the working stroke of the sealing elements and allows the single-stage PPG to achieve a flow capacity characteristic of significantly more complex two-stage systems. The theoretical justification for the proposed methodology is based on a developed dynamic model, where the hydraulic link is represented as a viscoelastic concentrated Kelvin-Voigt body. This approach has made it possible to adequately account for the elastic compressibility of the working fluid and dissipative losses, which is critical for precision small-scale vibration systems. The calculation algorithm involves the sequential determination of key geometric parameters (sealing stage diameters d_1 and d_2), the force characteristics of the elastic elements, and the parameters of the pumping station. It has been established that the key factors governing frequency are the flow rate of the working fluid and the stiffness of the PPG springs, which allows the drive parameters to be adapted to specific technological processes, such as powder vibro-compaction, vibro-abrasive machining and vibro-turning with chip grinding. The developed methodology serves as a tool for multi-criteria optimisation of HPD parameters at the design stage to achieve maximum energy efficiency and reliability.

Keywords: Vibrations, Hydraulic pulse drive, Pressure pulse generator, Slotted spring, Mathematical modelling, Kelvin–Voigt body, Oscillation frequency.

1. Introduction

Vibration-based process equipment, which is used in various sectors of industry and the national economy – for example, for the vibro-compaction of powder-based products, the rolling of bearing rings, the manufacture of casting moulds and reinforced concrete structures, and so on—is quite diverse, primarily due to the use of various types of vibrating drives (mechanical, pneumatic, hydraulic, electromagnetic, combined, etc.) [1 - 7]. An analysis of the advantages and disadvantages of these drives shows that, at present, the hydraulic impulse drive (HPD) offers significant advantages [2, 8], particularly the type featuring a control element in the form of a parametric pressure pulse generator (PPG), which generates and regulates the parameters of the vibration machine's operating cycle [1, 8]. The HPD provides any required operating forces (up to 320 kN and above) and a wide range of vibration parameter control (frequency – 1... 100 Hz, amplitude – (0.1...10)10^{-3} m) in the drive link of vibrating (VM) and vibro-impact (VIM) process machines; it is simple and reliable in operation and has a relatively low metal content.

In addition to the traditional vibration technologies mentioned above, as evidenced by an analysis of publications over the last few decades [9–11], there has been growing interest among

dx.doi.org/10.17683/ijomam/issue24.20

researchers and manufacturers in vibration-assisted cutting processes (turning, drilling, etc.) when machining materials with high strength, wear resistance, heat resistance, hardness, etc., where other methods are ineffective or economically unviable, and in the vibrational surface hardening of parts (VSH) through surface plastic deformation (SPD).

The technological capabilities of traditional (vibropresses, vibropress-hammers, etc.) VM and VUM systems based on PPG are closely linked to the technical characteristics of the PPG controlling their HPD, in particular the throughput capacity of the PPG, which can be increased in various ways – through the use of multi-stage PPGs [8] and others. Multi-stage PPGs are effective, but in the case of PPGs for hydro-pulse devices for vibro-cutting and VSH, they are structurally complex and have significant dimensions, particularly for large passage cross-sections (nominal passages). The development of hydro-pulse devices for vibro-cutting and VSH based on parametric single-stage PPGs, by combining their shut-off and power components (elements) with high-stiffness elastic elements of the slotted (SS) and annular springs [12 – 14], has enabled the development of compact devices which, unlike known mechanisms for the aforementioned material processing operations, can be installed, for example, in the tool holder of a turning and thread-cutting machine without altering its kinematic scheme or the design of the slide. The expansion of the technical and technological capabilities of hydraulic impulse machines and devices with single-stage PPGs based on SS or annular springs is linked to an increase in their throughput capacity.

One way of increasing the nominal flow capacity of parametric single-stage PPGs is to reduce the stroke of their shut-off elements by eliminating spool sealing (positive overlap) at both levels of change in the cross-sectional area of the shut-off elements and by using face (valve) sealing and short SS (or annular springs), the stiffness of which is determined at the limit of permissible stresses in the spring elements arising in the cross-sections of the SS (or annular springs) under their maximum possible loads.

The implementation of this design principle has made it possible to create parametric single-stage PPGs based on the combination of their shut-off elements with SS, which are close in flow capacity to two-stage generators. Designs of PPGs have been developed that can be connected to the actuators (hydraulic cylinders, hydraulic motors, etc.) of PPGs in both 'input' and 'output' configurations [1, 8], which significantly expands the scope of application of PPGs with this type of generator.

We will examine the development of a design calculation methodology for a hydraulic impulse drive controlled by a single-stage high-capacity hydraulic impulse valve, based on a configuration in which the hydraulic impulse valve is connected to the actuator hydraulic cylinder (AHC) 'at the inlet' [1], since the design equations obtained for this configuration can be used practically without modification or significant refinement for other configurations of PPG connection to the AHC.

2. Researches Methodology

A schematic diagram of a hydraulic pulse drive (HPD) with an integrated single-stage pressure pulse generator (featuring enhanced throughput capacity is shown in Figure 1. The system is implemented using an 'inlet' connection to the actuator hydraulic cylinder .

The structure of the pressure pulse generator includes a main housing 1, housing an internal liner 2 that contains the primary sealing unit 3. This unit is designed as a tapered valve integrated with a high-rigidity slotted spring. The conical segment of this shut-off component 3 interfaces with a valve seat 4, which is secured within the housing 1 via the liner 2 and an end cap 5. This assembly is fastened to the main body 1 using standard hardware, such as bolts or dowels, which are omitted from the diagram for clarity.

The second sealing level of the parametric PPG is achieved through a valve bushing 6 featuring a pair of tapered sealing bevels. The first of these (the bottom one in Fig. 1) interfaces with the primary bevel of the valve seat 4, while the second (the top one in Fig. 1) aligns with a corresponding tapered bevel machined into the internal cavity of the liner 2.

Valve sleeve 6 is guided by the cylindrical section of the valve body of the shut-off element 3, with which it is mated in diameter d_1' via a precise sliding fit, for example $d_1'H7/g6$, thereby ensuring a high degree of sealing in this direction at the moment the PPG opens, owing to the significant length of the mating surface.

The compression force of the helical spring 7 maintains the primary contact pressure between the polished lower bevels of the valve bushing 6 and the seat 4. This spring acts through a stepped collar 8, whose shank is aligned with the outer cylindrical surface of the valve bushing 6, functioning as a guide for spring 7. Along with the spring retaining washer 9, it holds the valve bushing 6 firmly against the bottom bevel of the seat 4. The opposite (top) end of spring 7 is seated against the base of the liner bore 2, which also serves as the seating surface for the upper tapered bevel of the PPG's second sealing stage.

To facilitate effective force transmission from the valve bushing 6 during the opening phase of the PPG, it is designed with a cylindrical stem. A structural clearance $h_a \le 0,5h_b$ is maintained between the end

of this stem and the shoulder of the shut-off component 3, where h_b represents the negative overlap, corresponding to the operational stroke of both the locking unit 2 and the valve bushing 6. To ensure the unhindered flow of the hydraulic medium from the B_{HD} chamber (which links the PPG to the A_{B1} working cavity of the actuator) to the executive cylinder, longitudinal through-slots *'b'* are machined into the stem of the valve bushing 6, as illustrated in the *B-B* section of Fig. 1.

To minimise potential energy losses when the PPG opens, a small positive overlap of $\approx 0{,}1h_b$ R is formed on the shank of the valve sleeve 6 near the upper sealing chamfer.

The initial compression y_{01} of the slotted spring (SS) with stiffness k_1 for the shut-off component 3 is modified using a plunger 10 located within the bore of the end cap 5.

This adjustment is performed by a regulating screw 11, which sets the 'opening' pressure p_1 of the PPG and is secured in place by a lock nut 12. Conversely, the pre-deformation y_{02} of the helical spring 7 (with stiffness $k_2 \ll k_1$) cannot be adjusted, as its value is fixed by the structural dimensions during the initial assembly of the generator.

The actuator of the parametric hydraulic pulse drive is a hydraulic cylinder comprising a housing (omitted from Fig. 1) and a multi-diameter (stepped) plunger 13. This plunger features a dual-stage sealing system: the primary stage utilizes a valve-type interface with a mean diameter d_3 of its tapered seat, whereas the secondary stage functions as a spool-type seal, achieved through the high-precision fit of the guiding segment with a diameter d_4 (representing the effective cross-sectional working area).

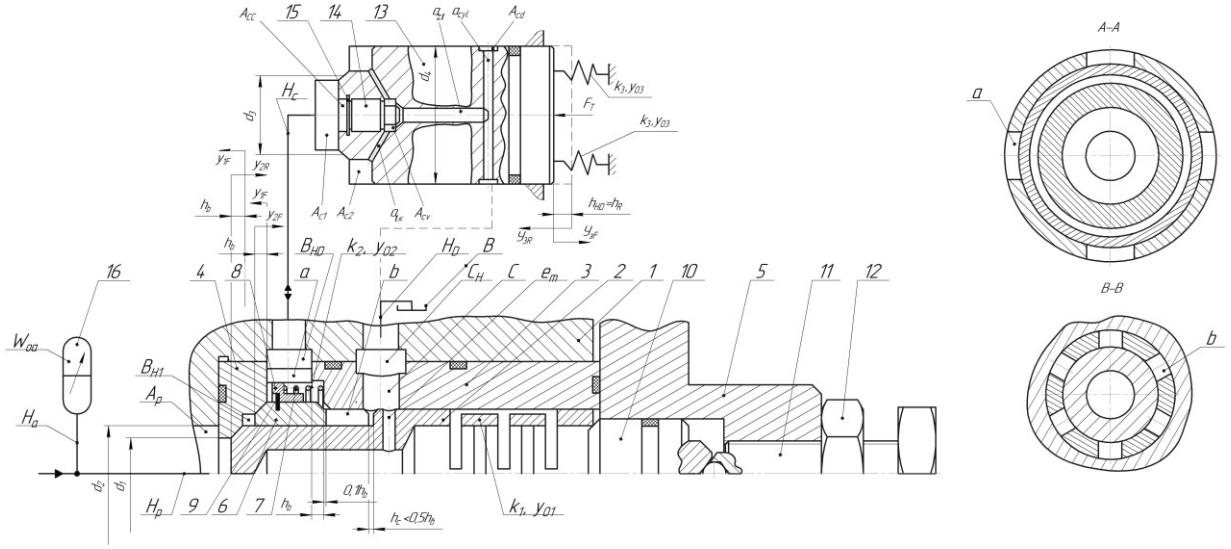

Figure 1: Block diagram of a hydraulic impulse drive controlled by a single-stage high-capacity hydraulic impulse valve

To ensure that the plunger 13 returns to its initial position during its return stroke, a valve-plunger 14 is fitted into the central axial bore of the valve section of the plunger 13; a conical chamfer is formed on the end face of the valve section, which is lapped against a seat machined at the bottom of this bore.

The base of the plunger valve 14 (as illustrated in Fig. 1) is supported by a spring washer 15. The A_{CC} chamber, which serves as an extension of the plunger valve's central longitudinal bore, maintains an open connection with the A_{C1} working cavity of the HPD cylinder's initial sealing stage. Simultaneously, the A_{C2} chamber of the second sealing stage is linked to the A_{CV} cavity within the valve portion of plunger 14 through a series of inclined 'a_{tk}' channels.

In the default state of the plunger valve 14 (refer to Fig. 1), the A_{CV} chamber is linked to the reservoir via the 'a_{zt}' and 'a_{zd}' ports and the A_{CD} recess. Beyond their primary role, the A_{CD} recess and 'a_{zd}' apertures serve as auxiliary drainage components, effectively preventing any external discharge of the hydraulic medium during the operation of the HPD.

The sleeve 2, saddle 4 and plunger 10 are sealed by circular rubber O-rings, which are not shown with reference numbers in Fig. 1.

The hydraulic medium is delivered from the pumping unit (omitted from Fig. 1) to the A_P pressure chamber of the PPG and the cyclic accumulator 16 via the H_P and H_a supply lines. The hydraulic accumulator 16 is characterized by an initial operating volume W_{0a}. The simplest cycle-type hydraulic accumulator is a reservoir whose capacity can be adjusted. The potential energy in such an accumulator is stored due to the compressibility of the working fluid.

The primary sealing stage of the parametric PPG is defined by the mean diameter of the polished chamfer 4 on the valve portion of the shut-off component 3. Correspondingly, the secondary sealing stage is determined by the mean diameters of the lower chamfer on seat 4 and the upper sealing bevel of the valve bushing 6, which is fitted against the seat within the liner bore. To avoid geometric complexities during the analytical calculation of the PPG caused by using mean diameters, the minimum cone diameters of the functional chamfers are adopted as the reference values: d_1 for the first stage and d_2 for the second (refer to Fig. 1). Since the width of these sealing surfaces is minimal (under 2 mm [12]), this simplification does not compromise the overall precision of the PPG performance evaluation.

At the starting phase, when the hydraulic medium pressure p_r is below the opening threshold p_1, the plunger 13 remains in its lowest position. This state is maintained by the combined effect of its own mass (as the HPD cylinders are typically oriented vertically in vibratory and vibro-impact machinery) and the force from return springs, represented in Fig. 1 as elastic components with stiffness k_3 and a pre-compression value of y_{03}. Consequently, the initial sealing stage makes contact with its seat at the mean diameter d_3.

In this configuration, the working chambers A_{C1} and A_{C2} are linked to the drain cavity C_H of the PPG via the H_C line, passing through the B_{HD} chamber, slots '*a*', the intermediate cavity B_{H2}, slots '*b*', and apertures '*c*' in the liner 2. This drain cavity is directly coupled to the reservoir *B* of the pump station through the H_D return line. Furthermore, the A_{C2} chamber's connection to the tank *B* is facilitated by the plunger valve 14, which stays open in its lower position due to gravity. The fluid path includes the 'a_{tk}' inclined port, the 'a_{zt}' main longitudinal bore, 'a_{zd}' radial apertures, the A_{CD} recess, and the H_{dr} drainage line.

The cavity housing the shut-off element 3 of the PPG is connected, via radial holes in it and holes '*c*' in sleeve 2, to the drain cavity of the PPG's C_H. The role of the closing-mode throttle can be performed by the clearance in the mating surface with diameter d_1^1 between the valve sleeve 6 and the cylindrical part (valve) of the PPG shut-off element 3. If, during the adjustment of the PPG operating mode, it is found that the clearance is insufficient, then the effect of the clearance may be enhanced by means of a groove (or grooves) formed mechanically (by cutting, grinding, etc.) on the mating surface of the valve sleeve 6 and the valve part of the shut-off element 3 along the diameter d_1^1 (on the valve sleeve 6 or the shut-off element 3).

3. Results and Discussion

The main initial data for developing a design calculation method for the high-capacity HPD and PPG, connected to the HPD actuating hydraulic cylinder (see Fig. 1) in an 'inlet' configuration [3], include:

– the nominal pressure of the working fluid during PPG opening p_1 ('opening pressure');

– the type of hydraulic pump in the HPD pump-accumulator station – a gear-type hydraulic pump, as hydraulic pumps of this type operate most reliably and stably in the PPGI due to the absence of suction and discharge valves. Since the flow rate Q_{pump} of the hydraulic pump is a calculated value, the specific model of the required hydraulic pump is selected after determination Q_{pump};

– the adjustment range of the PPG and HPD parameters:

– the frequency of pressure pulses in Hz (it is assumed that the frequency range of the vibrations of plunger 13 of the HPD's actuating hydraulic cylinder (see Fig. 1) is the same);

– vibration amplitudes of plunger 13 (see Fig. 1) – $(0,5...2)\cdot 10^{-3}$;

– adjustment range for the pre-deformation of the elastic elements of the PPG and HPD (see Fig. 1): SS – y_{01}; coiled spring 7 – $y_{02\max}$ (a constant initial deformation is created during the assembly of the PPG); elastic elements returning the plunger to its initial position 13 – y_{03} (the value of y_{03} depends on the specific type of HPD);

– the approximate pressure rang $\Delta p = p_1 - p_2$, , which depends on the internal transmission ratio $u_{21} = A_1^2 \cdot A_2^{-2} = d_1^4 \cdot d_2^{-4}$ [1, 8]. We will book an appointment in advance: $u_{21}^{0,5} = 0,3...0,5$; ($u_{21} = 0,55...0,71$ [8]).

– the type of energy source, which determines the type and variety of control and distribution hydraulic equipment and HPD hydraulic fittings;

-– the approximate value of the volume W_0 of the pressure chamber of the HPD;

– the approximate maximum stroke of plunger 13 (see Fig. 1) h_R should be taken as equal to the maximum vibration amplitude, since the vibrational displacement $y_{3F} = y_{3R}$ occurs in the additional coordinate direction y_R during the zero cycle;

– approximate values of the reduced masses m_1, m_2 and m_3 including their components;

– the maximum process force F_T, as determined by the characteristics of the process being carried out using the HPD under investigation;

– permissible flow velocities of the working fluid in the pressure [V_H] and discharge [V_{dr}] hydraulic lines of the PPG and HPD, for example, in the

hydraulic lines H_p, H_f, H_c, H_{DR}, H_D and ports a_{tk}, a_{zt} and a_{zd} (see Fig. 1);

– accuracy grades for the mating surfaces of the sealing elements of the first and second sealing stages of the PPG and the plunger 13 of the HPD actuating hydraulic cylinder (see Fig. 1);

– material grades (steel) of the main components of the PPG, plunger 13 and plunger valve 14, and the recommended surface hardness ranges for these components (see Fig. 1), for example:

– locking element 3 – 60C2A steel (DSTU 8429:2015), 47–50 HRCe;

– seat 4 – 100Cr6 steel in accordance with DSTU ISO 683-17, 62…64 HRCe;

– sleeve 2 – 100Cr6 steel in accordance with DSTU ISO 683-17, 62…64 HRCe;

– valve sleeve 6 – 100Cr6 steel in accordance with DSTU ISO 683-17, 62–64 HRCe;

– plunger 13 – 20X steel in accordance with DSTU 7806:2015, 56–62 HRCe (case-hardened);

– methods of connecting components and links of the HPD and PPG systems.

The materials for other components of the PPG and HPD are selected during the design of the PPG and HPD based on an analysis of their intended use and operating conditions.

In addition to the basic initial data listed above, which are necessary for the development of a scientifically sound methodology for the design calculation of the PPG and HPD under investigation, additional clarifying data may be introduced where necessary.

Experimental studies of the HPD [1, 4, 5] have shown that this actuator consumes the most power at high pressure pulse frequencies $\nu_{\max}$. Assuming that the oscillations (vibrations) of the plunger 13 of the HPD actuating hydraulic cylinder are close to harmonic, the total energy of the harmonic oscillations [12] $E_b = 0,5m_3h_{3\max}^2\omega_{\max}^2 = 2\pi^2 m_3 h_{3\max}^2 \nu_{\max}^2$ is equal to the average work $\overline{A}_{VT}$ done by the pressure forces during the movement of plunger 13 along its forward and return strokes (see Fig. 1): $\overline{A}_{VT} = 0,5 \cdot p_1 \cdot h_{3\max} \cdot A_3$ [13]. The given relationships specify the maximum values of the frequency of pressure pulses and the displacement of the plunger 13, and take into account that $\omega_{\max} = 2\pi\ \nu_{\max}$ – the angular frequency of pressure pulses during the vibration of the plunger 13.

The initial position of the plunger 13 is not the equilibrium position assumed for harmonic oscillations, such as those of a pendulum; therefore, the oscillatory motion of the plunger 13 can be regarded as the positive half of a harmonic oscillatory process, the amplitude of which is h_3, whilst the pressure in chambers A_{c1} and A_{c2} (see Fig. 1) varies according to a pulsating harmonic law with amplitude $\Delta p = p_{1\max}$. Based on the above considerations and assumptions, in [3] the following formula was derived from the equality $E_b = \overline{A}_{VT}$ for calculating the cross-sectional area of the plunger of the actuating hydraulic cylinder, i.e. plunger 13:

$$A_3 = 39,48 \cdot m_3 \cdot h_{3\max} \cdot \nu_{\max}^2 \cdot p_{1\max}^{-1}. \quad (1)$$

Since, according to the accepted basic initial data, the type of cyclic hydraulic accumulator is of the variable-capacity type, where the potential energy for the pressure pulse supplied through the open hydraulic line into cavities A_{c1} and A_{c2} (see Fig. 1), is stored due to the compressibility of the working fluid $\Delta W_{\max}$, the maximum volume of the working fluid supplied to these chambers under pressure $\Delta p = p_1 - p_2$ is determined by the relationship given in [12]:

$$\Delta W_{\max} = h_{3\max} \cdot A_3 \cdot \kappa \Big/ \left[K_3 \cdot p_1 \left(1 - u_{21}^{0,5}\right)\right], \quad (2)$$

where $K_3 = 1,0...1,5$ – a safety factor that guarantees account is taken of the possible inertial motion of the plunger 13 (see Fig. 1) under maximum process resistance and the resistance of the elastic forces (neglecting friction forces). The value $K_3 = 1,0$ is taken when the inertial component is neglected during h_3. These resistance forces $F_{\max}$ can be estimated using the approximate relationship:

$$F_{\max} = 2k_3 \left(y_{03} + h_3\right) + F_{T\max} + m_3 g), \quad (3)$$

where $F_{T\max}$ – the maximum possible force exerted by the technological resistance of the object being acted upon by the actuating hydraulic cylinder.

The minimum amplitude $h_{3\min}$ of the plunger's vibrations 13 will be given by $W_{0\Sigma} = W_0 + W_{0a} = W_0$. ($W_{0a} = 0$), whereas, when the cyclic hydraulic accumulator is operating, only the initial volume W_0 of the pressure chamber of the HPD is utilised, $h_{3\max}$ and $W_{0a\max}$ will be given by . Based on formula (2) and the observations made, we can write:

$$\Delta W_{\min} = h_{3\min} \cdot A_3 \cdot \kappa \Big/ \left[K_3 \cdot p_1 \cdot \left(1 - u_{21}^{0,5}\right)\right]; \quad (4)$$

$$W_{0\Sigma\max} = W_0 + W_{0a\max}. \quad (5)$$

On the other hand, in cyclic hydraulic accumulators, which store potential energy solely through the compressibility of the working fluid, the following relationships hold true [3]:

$$\Lambda W_{\max} = W_{0\Sigma\max} \cdot p_{1\max} \cdot (1 - u_{21}^{0,5}) \cdot \kappa^{-1}; \quad (6)$$

$$\Lambda W_{\min} = W_0 \cdot p_{1\max} \cdot (1 - u_{21}^{0,5}) \cdot \kappa^{-1}; \quad (7)$$

Taking (2) and (3) into account, after some straightforward algebraic manipulations, we obtain:

$$W_{0a\max} = W_0(h_{3\max}/h_{3\min} - 1); \quad (8)$$

Substituting (8) into (5), we find:

$$W_{0\Sigma\max} = W_0 \cdot h_{3\max}/h_{3\min}. \quad (9)$$

Comparing $\Delta W_{\min}$ (7) with (4), we find that:

$$W_0 = h_{3\min} \cdot A_3 \cdot \kappa^2 \cdot K_3^{-1} \cdot p_{1\max}^{-1} \cdot (1-u_{21}^{0,5})^{-2}; \quad (10)$$

The flow capacity of the PPG is determined by the cross-sectional area A_1 of the first section of the PPG's sealing stage (see Fig. 1).

The diameter d_1 is effectively the diameter d_{ym} of the PPG's nominal passage; to determine this, it is necessary to know the flow rate Q_{pump} of the hydraulic pump in the HPD pump-accumulator station. The theoretical flow rate Q_{pump}^{teor} can be calculated using the formula [1, 8, 12] known for the HPD [3]

$$Q_{pump}^{teor} = K_{tsa} \cdot v_{\max} \cdot p_{1\max} \cdot W_{0\Sigma\max} \cdot \kappa^{-1} \cdot \eta_{OH}^{-1}, \quad (11)$$

where K_{tsa} – cyclic pressure pulse coefficient (see equation (7)); η_{OH} – volumetric efficiency of the hydraulic pump (for gear pumps $\eta_{OH} = 0,95...0,96$ [15]). The cycle diagram of the HPD operating cycle (see Fig. 2) is indicative (of a conventional nature), which defines K_{tsa} as an estimate, and this requires the introduction of a safety factor K_{zn} into equation (12), the value of which can be refined on the basis of theoretical and experimental studies of HPD and PPG. It is preliminarily recommended [12, 14] to take $K_{zn} = 1,1...1,25$, in which case equation (11) will take the form:

$$Q_{pump} = K_{zn} \cdot Q_{pump}^{teor} = K_{zn} \cdot K_{tsa} \cdot v_{\max} \cdot p_{1\max} \cdot W_{0\Sigma\max} \cdot \kappa^{-1} \cdot \eta_{OH}^{-1} =$$

$$= K_{zn} \cdot K_{tsa} \cdot v_{\max} \cdot p_{1\max} \cdot W_0 \cdot h_{3\max} \cdot \eta_{3\min}^{-1} \cdot \kappa^{-1} \cdot \eta_{OH}^{-1} = \quad (12)$$

$$= K_{zn} \cdot K_{tsa} \cdot v_{\max} \cdot h_{3\max} \cdot A_3 \cdot \kappa \cdot p_{1\max}^{-1} \cdot (1-U_{21}^{0,5})^{-2} \cdot K_3^{-1} \cdot \eta_{OH}^{-1};$$

or taking into account the values K_{zn} i K_3.

$$Q_{pump} = (0,78...1,18) \cdot K_{tsa} \cdot v_{\max} \cdot h_{3\max} \cdot A_3 \cdot \kappa \cdot p_{1\max}^{-1} \cdot (1-U_{21}^{0,5})^{-2} \cdot \eta_{OH}^{-1}, \quad (13)$$

where the average value of the ratio is given $K_{zn}/K_3 = 0,78...1,18.$

The discharge of the cyclic hydraulic accumulator 16 from chambers A_{c1} i A_{c2} of the HPD actuator cylinder takes place over a time interval $t_{RT} = t_{HC} + t_{CB}$, causing the plunger 13 to move by a distance h_3 and remain in the upper position for a duration of $t_{PP} + t_{pB}$, with the displacement of the plunger 13 by a distance h_3 lasting for a time $t_{pp} = t_{HC} - t'_{HC}$ (see Fig. 1). From the approximate cycle diagram of the HPD operating cycle (see Fig. 2), it is evident that the duration of the full pressure pulse in the pressure chambers A_{c1} and A_{c2} of the HPD actuator hydraulic cylinder (see Fig. 1) corresponds to the duration of the discharge of the cyclic hydraulic accumulator 16 as follows:

$$t_{zn} + t_{HT} = t_{HC} + t_{CB} + t_{CZ}. . \quad (14)$$

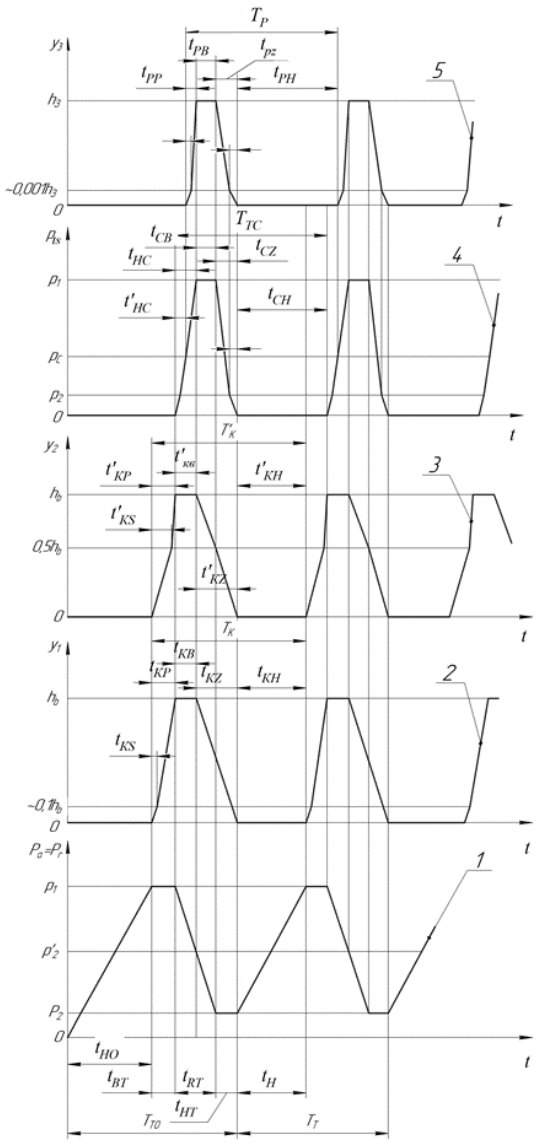

Figure 2: Approximate cycle diagram of the working cycle of a hydraulic pulse drive controlled by a high-capacity pressure pulse generator: 1 – pressure change curve in the pressure chamber A_p of the PPG and the cyclic hydraulic accumulator 16; 2 – movement curve of the locking element 3 PPG; 3 – valve bushing displacement curve 6; 4 – pressure change curve in cavities AC1 and AC2 executive hydraulic HPD; 5 – plunger curve 13 of the executive hydraulic cylinder

The time t_H taken for pressure to build up in the A_H pressure chamber and hydraulic accumulator 16 (see Fig. 1) can be estimated most accurately using the known relationship [8, 13]:

$$t_H = \frac{\Delta p \cdot W_{0\Sigma}}{\kappa \cdot Q_{pump}}, \quad (15)$$

where κ – the isothermal modulus of elasticity of the energy carrier.

The pressure of the working fluid decreases from p_1 to $p_2$over a period of time t_{RT}, which allows this time to be estimated using an equation similar to (15):

$$t_{RT} = (p_1 - p_2) \cdot W_{0\Sigma} / \left(Q_{mg} \cdot x\right), \quad (16)$$

where Q_{mg} – average flow rate of the energy carrier through the open slot in the PPG A_{CPPG} (see Fig. 1).

Assuming that the function $p_r = f(t)$ [14] is approximately linear, comparing (15) and (16) we find:

$$Q_{mg} = Q_{pump} \cdot t_H / t_{RT} = Q_{pump} \cdot \tau_{RT}, \quad (17)$$

where $\tau_{RT} = t_H / t_{RT}$ – the relative time taken for the pressure of the working fluid in the cyclic accumulator 16 (see Fig. 1) to decrease from level p_1 to level p_2 (see Fig. 2). According to the cycle diagram of the HPD operating cycle (see Fig. 2) $t_{RT} < t_H$ ($t_{RT} > 1$),, from which it follows that $Q_{mg} > Q_{pump}$.

In order to avoid adverse effects, such as cavitation, during the operation of the hydraulic motor and the parametric actuation of the AHC HPD, and in accordance with the design rules for hydraulic drives [12], the average velocity V_{mg} of the working fluid through the open orifice A_{CPPG} of the PPG must not exceed the permissible value $[V_{h2}]$:

$$V_{mg} = Q_{mg} / \left(\pi d_2 h_b\right) \le \left[V_{h2}\right] \quad (18)$$

where

$$Q_{mg} \le \pi d_2 h_b \cdot \left[V_{h2}\right]. \quad (19)$$

If we disregard any potential internal energy losses in the PPG and the HPD actuating hydraulic cylinder, then when the PPG is open and the cycle hydraulic accumulator 16 is being discharged (see Fig. 1), a flow of energy carrier Q_{mg} passes through the flow cross-section A_1, the velocity V_m of which must also not exceed the permissible value $\left[V_{h1}\right] = \left[V_{h2}\right]$:

$$V_{h1} = Q_{mg} / A_1 = 4Q_{mg} / \left(\pi d_1^2\right) \approx 1,274 Q_{mg} d_1^{-2} \le \left[V_{h1}\right]. \quad (20)$$

It was noted above that the diameter d_1 of the first sealing stage of the PPG is in fact the diameter d_{ym} of the nominal bore of the PPG, which can be found using equation (20):

$$d_{ym} = d_1 \ge \left(4Q_{mg} / \pi\left[V_{h1}\right]\right)^{0,5} \approx 1,13\left(Q_{mg} / \left[V_{h1}\right]\right)^{0,5} \approx$$
$$\approx 1,13\left[\left(Q_{mg} \cdot \tau_{ZT}\right) / \left[V_{h1}\right]\right]^{0,5}. \quad (21)$$

By taking the limit in inequality (29) and equating the resulting expression with (17), we find the relative time

$$\tau_{ZT} = \pi d_2 h_b \left[V_{h2}\right] / Q_{pump}. \quad (22)$$

Substituting (22) into (21) yields a simple formula relating the internal diameters d_1 and d_2 of the cross-sections of the first and second sealing stages of the PPG, respectively, to the stroke h_b of their sealing elements (see Fig. 1):

$$d_1 \ge (d_2 \cdot h_b)^{0,5}. \quad (23)$$

It is evident that, whilst the shut-off element 3 and the valve sleeve 6 are moving, only a fluid friction regime occurs in the clearances of their guideways (see Fig. 1). According to the approximate cycle diagram of the HPD operating cycle (see Fig. 2), the energy balance of the forward stroke of the sealing elements and the second sealing stage of the PPG (sealing element 3 and valve sleeve 6) can be described by the equation:

$$A_{mp} = \Delta E_{ss} + \Delta E_{HP} + \Delta E_{HL} + A_f, \quad (24)$$

where $A_{mp} = p_{1\max} \cdot h_b \cdot A_2$. (25)

the average work done by the working fluid's pressure forces during the $t_{KP} + t_{KB}$ (or $t'_{KP} + t'_{KB}$) forward stroke of the shut-off element 3 together with the valve sleeve 6 (see Fig. 1 and Fig. 2);

$$\Delta E_{SS} = 0,5 \cdot k_1 \cdot h_b^2 \quad (26)$$

– the increase in the potential deformation energy of the locking element 3;

$$\Delta E_{HP} = 0,5 \cdot k_2 \cdot h_b^2 \quad (27)$$

– device for measuring the potential energy of a coiled spring 7;

$$A_f = F_{f1} \cdot h_b. \quad (28)$$

– the total average work done by the frictional forces during the linear movement of the locking element 3 and the valve sleeve 6;

$$\Delta E_{HL} = 0,5 \cdot k_{or} \cdot x_{01}^2 = 0,5 \cdot p_{1\max}^2 \cdot A_0^2 \cdot k_{or}^{-1}. \quad (29)$$

– the increase in the potential deformation energy of the elastic part of the hydraulic link (HL) of the HPD

[12 - 14], де: $A_0 = \sum_{i=n}^{i=n}(l_i \cdot A_i) \Big/ \sum_{i=n}^{i=n} l_i$ (here $l_i \cdot A_i$ – accordingly, the length and cross-sectional area of the *i*-th hydraulic channel and hydraulic line of the combined head cavity of the PPG and HPD, etc.) – the cross-sectional area of the average hydraulic line of the HL; $k_{or} = A_0^2 \cdot \kappa \cdot W_{0\Sigma\max}^{-1}$ – stiffness HL; $x_{01} = p_1 A_0 \cdot k_{or}^{-1}$ – the linear deformation of the HL corresponding to the pressure p_1 'opening' of the PPG.

Since $k_2 \square\ k_1$, and as already noted, the friction regime in the clearances between the locking element 3 and the valve sleeve 6 is fluid friction, the terms ΔE_{HP} and A_f can be neglected; equation (24) will then take the form

$$A_{mp} \geq \Delta E_{SS} + \Delta E_{HL} \tag{30}$$

or taking into account (25), (26) i (29)

$$p_{1\max} \cdot h_b \cdot A_2 \geq 0,5 \cdot k_1 \cdot h_b^2 + 0,5 \cdot p_{1\max}^2 \cdot A_0^2 \cdot k_{0r}^{-1} =$$

$$= 0,5(k_1 \cdot h_b^2 + p_{1\max}^2 \cdot \kappa^{-1} \cdot W_{0\Sigma\max}), \tag{31}$$

where

$$A_2 \geq 0,5(k_1 \cdot h_b \cdot p_{1\max}^{-1} + p_{1\max} \cdot x^{-1} \cdot h_b^{-1} \cdot W_{0\Sigma})^{0,5}, \tag{32}$$

or

$$d_2 \geq 0,798 \cdot (k_1 h_b p_{1\max}^{-1} + p_{1\max} \cdot x^{-1} \cdot h_b^{-1} \cdot W_{0\Sigma})^{0,5} \tag{33}$$

where the symbol «≥» in (30) accounts for the neglect of the quantities ΔE_{HP} and A_f; $A_2 = \pi d_2^2 / 4 \approx 0,785 d_2^2$; for the values of k_{or} and A_0 – see the explanation in (59).

When calculating the moving mass m_1 for *SS* the shut-off element 3 (see Fig. 1), a number of assumptions were made, on the basis of which a formula was derived in [12, 13] for calculating the equivalent stress $\sigma_{екв}$ in the critical cross-sections of the working rings of the shut-off element *SS*:

$$\sigma_{екв} = (1,22 \cdot F_{SS} \cdot R) \cdot a^{-3} \leq [\sigma], \tag{34}$$

where $F_{SS} = k_1 \cdot h_b \approx p_1 \cdot A_2$ – maximum load applied to the *SS*; *R* and *a* – geometric parameters of the structural element [18]. In the above-mentioned paper [14], a simplified formula for calculating the stiffness k_1 of the *SS* was also derived:

$$k_1 = 1,035 \cdot E \cdot a^4 / (R \cdot n), \tag{35}$$

where $E = 2,15 \cdot 10^5$ MPa – modulus of elasticity *SS* (steel 60C2A DSTU 8429:2015).

Setting $\sigma_{екв} = [\sigma]$ in (64), we obtain from equations (34) and (35) the expressions for the ultimate load $F_{SS\max}$ at which the strength of the structural element is ensured and its maximum deformation $h_{SS\max}$ is achieved: [12, 13]:

$$F_{SS\max} = 0,82[\sigma] \cdot a^3 \cdot R^{-1}; \tag{36}$$

$$h_{SS\max} = 0,79[\sigma] \cdot n \cdot R^2 \cdot E^{-1} \cdot a^{-1}. \tag{37}$$

Substituting equations (35) and (37) into (33) for $h_{SS\max} = h_b$, and after performing the algebraic manipulations, we obtain

$$d_2 \geq 0,722 \left\{ \frac{[\sigma] a^3}{R \cdot p_{1\max}} \left[\frac{1 + 1,548(p_{1\max} \cdot E \cdot W_{0\Sigma\max})}{\kappa [\sigma]^2 \cdot n \cdot R \cdot \pi^2} \right] \right\}^{0,5}. \tag{38}$$

It is advisable to reconcile the value of the diameter d_2 obtained from (38) with equation (18) and, for design and manufacturing reasons, to assume that $d_2 = D_{3nn}$ (Fig. 3).

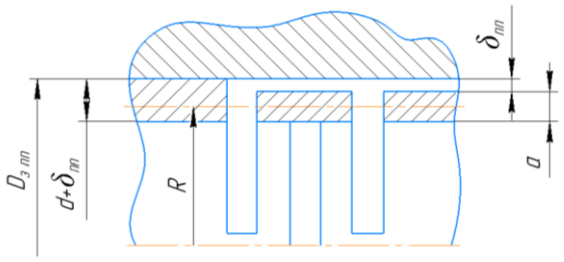

Figure 3: Determining the diameter d_2 of the second sealing stage of the PPG

If the clearance δ_{nn} between the mounting hole *SS* and the working part of this spring is ignored, then $d_2 = 2R + a$.

The required working stroke h_b of the shut-off element 3 and the valve sleeve 6 can be found from (23):

$$h_b \leq d_1^2 / d_2 . \tag{39}$$

The diameter d_4 of the 13 AHC HPD plunger is determined using the known relationship [12] from equation (1):

$$d_4 = \left(4A_3 / \pi \right)^{0.5} = 1,13 \cdot A_3^{0,5}. \tag{40}$$

The AHC HPD will perform its function most effectively in resonance mode, which is set conditionally for the HPD under investigation [11].

$$\omega_{\Sigma 3} = \sqrt{\omega_{p2}^2 \cdot u_{03} + 2\omega_{03}^2} \geq \sqrt{2} \cdot 2\pi \cdot v_{\max} = 8,88 v_{\max}, \tag{41}$$

where $\omega_{\Sigma 3}$ – natural frequency of the system's oscillations: the actuator hydraulic cylinder – HL;

$\omega_{03} = \sqrt{k_3 \cdot m_3^{-1}}$ – natural frequency of the mass m_3, loaded with elastic elements of stiffness k_3 (see. Fig. 1); $u_{03} = A_3^2 \cdot A_0^{-2}$ – the transmission ratio from the HL to the mass m_3 [3, 8]; $\omega_{P2} = \sqrt{k_{or} \cdot m_3^{-1}}$ – the natural frequency of a HL relative to its mass m_3.

Solving inequality (41) with respect to k_3 and substituting the values of the quantities described above, we obtain

$$k_3 \geq 39,43 \cdot m_3 \cdot v_{\max}^2 - \kappa \cdot A_3 \cdot W_{0\Sigma\max}^{-1}. \quad (42)$$

Using similar reasoning, we derive a formula for calculating the stiffness of coil spring 7 (see Fig. 1) based on the condition of its resonant operation:

$$\omega_{02} = \sqrt{k_2 \cdot m_2^{-1}} \geq \sqrt{2} \cdot 2\pi \cdot v_{\max} = 8,88 v_{\max}, \quad (43)$$

where:

$$k_2 \geq 8 \cdot \pi^2 \cdot m_2 \cdot v_{\max}^2 \approx 78,85 \cdot m_2 \cdot v_{\max}. \quad (44)$$

We can determine the initial F_{07} and working forces F_{P7} of spring 7 using simple formulas:

$$F_{07} = k_2 \cdot y_{02\max};\ F_{P7} = k_2 \cdot (y_{02\max} + h_b); \quad (45)$$

In accordance with the design specifications for the positioning of spring 7 in bore B_{H2} of the PPG on stepped sleeve 8 (see Fig. 1), the outer diameter D_7 and inner diameter d_7 of spring 7 are selected from the standard range of coil spring parameters, and all other parameters are calculated using a standardised method.

The value of the plunger diameter d_3 in the 13 parameter HPD AHC depends on the type of technological process being carried out by the VM or VIM with the HPD of the type under consideration. The diameter d_3 is most easily determined when the ratio p_c / p_1 or the intensity of the energy carrier pulses is specified [12]. If we assume $p_c \approx 0,5 p_{1\max}$ then, taking into account [16]:

$$p_c = \frac{4(2k_3 y_{03} + \bar{F}_{TO})}{(\pi d_3^2)} \approx 1,274(2k_3 y_{03} + \bar{F}_{TO}) d_3^{-2}, \quad (46)$$

we'll find:

$$d_3 \approx 1,596\left[\left(2 \cdot k_3 \cdot y_{03} + \bar{F}_{TO}\right) \cdot p_{1\max}^{-1}\right]^{0,5}. \quad (47)$$

The parameters of the elastic elements (coiled springs) for the return of plunger 13 (see Fig. 1) are determined in the same way as for spring 7.

Other structural dimensions of the PPG and HPD parts of the studied object are in the process of developing the design of the PPG and AHC HPD based on recommendations and experience in designing VM and VIM with HPD [1, 2, 3, 8].

In the work [1], the intensity I_p of the energy carrier pressure pulse, it is recommended to evaluate the dependence:

$$I_p = \Delta p / t_{imp}, \quad (48)$$

where $\Delta p = p_1 - p_2$, t_{imp} – pressure pulse duration. I_p in the international system of units (SI), it has the dimension Pa/s and, in physical terms, characterises the speed of the energy-force action of the energy carrier on the object of influence. The concept can be extended to the displacement pulses of the shut-off element 3, the valve sleeve 6 and the plunger 13, where, in terms of m/s, these intensities will characterise the speed of the PPG and HPD. By introducing the designation of the intensity of these displacement pulses in the directions y_1, y_2 and y_3, based on the cycle diagram of the working cycle (see Fig. 1 and Fig. 2), we obtain:

$$I_{KP} = h_b / (t_{KP} + t_{KB} + t_{KZ}) = h_B / t_{iKP}; \quad (49)$$

$$I'_{KP} = h_b / (t'_{KP} + t'_{KB} + t'_{KZ}) = h_B / t'_{iKP}; \quad (50)$$

$$I_{PP} = h_3 / (t_{PP} + t_{PB} + t_{PZ}) = h_3 / t_{iPP}; \quad (51)$$

where I_{KP}, I'_{KP}, I_{PP} – the intensity of displacement pulses, respectively, of the locking element 3, the valve sleeve 6, and the plunger 13 (see. Fig. 1); $t_{iKP} = t_{KP} + t_{KB} + t_{KZ}$, , $t'_{iKP} = t'_{KP} + t'_{KB} + t'_{KZ}$, , $t_{iPP} = t_{PP} + t_{PB} + t_{PZ}$, – duration of pulses of movement of the moving links of the PPG and the hydraulic cylinder of the HPD in the directions y_1, y_2 and y_3.

Intensity of energy carrier pulses in a hydraulic accumulator 16 I_{pa} and in the working cavities A_{C1} and A_{C2} of the hydraulic cylinder 16 I_{pts} HPD:

$$I_{pa} = \Delta p / \left(t_H + t_{BT} + t_{ZT}\right) = \Delta p / t_{ipa}; \quad (52)$$

$$I_{pts} = p_1 / \left(t_{HC} + t_{CB} + t_{CZ}\right) = p_1 / t_{ipts};; \quad (53)$$

where $t_{ipa} = t_H + t_{BT} + t_{ZT}$, $t_{ipts} = t_{HC} + t_{CB} + t_{CZ}$ – the duration of pressure pulses of the energy carrier in the hydraulic accumulator 16 and in the working chambers A_{C1} and A_{C2} of the hydraulic cylinder.

The plunger 13 (see Fig. 1) is accelerated by the pressure pulse in the working chambers A_{C1} and A_{C2} of the HPD executive hydraulic cylinder with an amplitude of $\Delta p' = p_1 - p_c$ and a duration of $t'_{ipts} = \left(t_{HC} - t'_{HC}\right) + t_{CB} + (t_{CZ} - t'_{CZ}) = t_{HC} + t_{CB} + t_{CZ} - (t'_{HC} + t'_{CZ}) =$ $= t_{ipts} - \Delta t_{ipts}$ (where $t_{ipts} = t'_{HC} - t'_{CZ}$ – decrease in the duration of the pressure pulse t_{ipts} due to the parametric principle of operation of the HPD executive hydraulic cylinder). The intensity of the energy carrier pressure pulse in the plunger acceleration section 13, by analogy with (52), will be

$$I'_{pts} = \Delta p' / t'_{ipts}. \quad (54)$$

The higher intensity of the pressure pulse of the energy carrier in the HPD hydraulic cylinder compared to the intensity of the pressure pulse in the cyclic hydraulic accumulator 16 (see Fig. 1) can be determined by dividing (54) by (51):

$$I'_{pts} / I_{pa} = (\Delta p' \cdot t_{ipa}) / (\Delta p \cdot t'_{ipts}), \qquad (54)$$

where

$$I'_{pts} = I_{pa}\left[(\Delta p' \cdot t_{ipa}) / (\Delta p \cdot t'_{ipts})\right]. \qquad (55)$$

For analysis (55), considering that $p_1 > p_c > p_2$, let us assume $p_c \approx 0,5 p_1,$, then $\Delta p' / \Delta p = 0,5 / (1 - p_2 / p_1)$. According to the data in [9], $p_2 / p_1 = 0,3 \ldots 0,6$. Taking the average value $(p_2 / p_1)_{\text{average}} = 0,91.$ and substituting it into (28), we obtain:

$$I'_{pts} = 0,91 \cdot I_{pa}\left(\frac{t_{ipa}}{t'_{ipts}}\right) = 0,91 \cdot I_{pa}\frac{t_H + t_{BT} + t_{ZT}}{t_{HC} + t_{CB} + t_{CZ} - \Delta t_{ipts}} =,$$

$$= 0,91 \cdot I_{pa}\frac{t_H + t_{BT} + t_{ZT}}{t_{BT} + t_{ZT} - \Delta t_{ipts}} \approx 1,82 \cdot I_{pa}, \qquad (56)$$

where it is customary $t_{HT} \approx t_{BT}$; $t_{ZT} + t_{HT} = t_{ipts}$, $t_H \approx t_{BT} + t_{ZT}$ (see. Fig. 2) and $\Delta t_{ipts} \approx 0$. A preliminary assessment of the levels of I'_{pts} and I_{pa} according to (56) shows that the intensity of I'_{pts} is almost twice that of I_{pa}.

Table 1 presents an example of results obtained using the developed methodology for the design calculation of a hydro-pulse drive controlled by a single-stage high capacity pressure pulse generator.

Table 1. Design parameters of the HPD based on a single-stage PPG (Calculation example)

Parameter	**Symbol**	**Unit**	**Value**
Input Data & Pump			
PPG opening pressure	p_1	MPa	16,0
Theoretical pump flow rate	Q_{Ht}	l/min	119,57
Cyclic fluid volume	ΔW	mm^3	36600
PPG Geometry			
1st stage diameter (nominal)	d_1	mm	13,0
2nd stage sealing diameter	d_2	mm	20,0
Operational stroke	h_b	mm	2,1
Actuator Parameters			
Plunger cross-sectional area	A_3	mm^3	1875
Plunger diameter	d_3	mm	50,0
Vibration amplitude (stroke)	h_3	mm	1,0
Elastic Elements			
Slotted spring stiffness	k_1	kN/m	78,8
SS pre-deformation	y_{02}	mm	26,8
Return spring stiffness	k_3	kN/m	493,0
Efficiency Metrics			
Operating frequency	f	Hz	50,0
Pulse intensity ratio	$\frac{I'_{pts}}{I_{pa}}$	—	1,82

The practical application of the developed methodology, using a supply pressure of 16 MPa and a flow rate of 110 l/min, demonstrates the high efficiency of the single-stage PPG with integrated slotted springs (SS). The calculation shows that a nominal passage diameter (d_1) of 13 mm is sufficient to ensure stable operation without cavitation, maintaining flow velocities within the permissible limit of 15 m/s. As shown in the results, the pressure pulse intensity in the actuator's working chamber (I'_{pts}) reaches 1,82 times the intensity of the power source (I_{pa}). This intensification is achieved through the transition to valve-type sealing and the minimization of the operational stroke (h_b = 2,1 mm, which drastically reduces inertial delays compared to traditional spool-type systems. The determination of the slotted spring stiffness (k_1 = 78,8 kN/m) and the return spring stiffness (k_3 = 493 kN/m) ensures that the system operates in a resonant mode at the target frequency of 50 Hz. This resonance is critical for minimizing energy consumption while maximizing the vibration amplitude (h_3 = 1 mm).

The developed methodology thus offers a comprehensive tool for the multi-criteria optimization of hydraulic impulse drives, balancing power density with structural reliability.

4. Conclusions

The construction of an indicative cyclogram (see Fig. 2) of the operating cycle of the HPD under investigation simplifies the establishment of sequential logical relationships between the dynamic processes in the drive (the movements of the moving parts of the PPG and the AHC of the HPD as a function of changes in the deformation (energy carrier pressure) of the HL) and the numerical relationships between the energy, force and geometric parameters of the HPD and PPG.

The concepts of pressure pulse intensity and displacement of the PPG and HPD components should be utilised in the design of VM and VIM systems incorporating HPD, the dynamic parameters of which must best meet the requirements of specific vibration technologies.

The methodology developed for the design calculation of the HPD and PPG enables all the main energy, force and geometric parameters of the PPG and the HPD's AHC to be determined using simple relationships.

In order to improve the reliability and accuracy of the calculation formulas and relationships set out in the methodology developed for the design calculation of the HPD and PPG under investigation, correlation coefficients obtained from theoretical studies of the mathematical model of the HPD under investigation, a controlled PPG with increased throughput capacity, may be introduced into them after the correctness and adequacy of this model have been verified by experimental studies of prototype PPG and HPD samples.

References

[1] R. Iskovych-Lototskyi, Fundamentals of the theory of calculation and development of processes and equipment for vibro-impact pressing: monograph. Vinnytsia: VNTU, 2006

[2] R. Iskovych-Lototskyi, O. Manzhilevskyi, and I. Sevostianov, "Analysis of advantages and disadvantages of different types of vibrating drives," in *Hydraulic impulse drives*, Vinnytsia: VNTU, 2013.

[3] M. Virnyk, R. Iskovych-Lototskyi, and N. Veselovska, Vibration and vibration-impact processes and machines in the foundry industry: monograph. Vinnytsia: VNTU, 2007.

[4] I. V. Sevostianov, Technology and equipment for vibro-impact dehydration of wet dispersed materials: monograph. Vinnytsia: VNAU, 2020.

[5] A. Maslov, Y. Salenko, V. Shchetinin, R. Vakulenko, and I. Kalach, "Theoretical Research of Vibrations of the Electromechanical Drive of a Technological Machine in Construction Production," 2021.

[6] G. Cieplok, "Self-synchronization of drive vibrators of an antiresonance vibratory conveyor," Journal of Theoretical and Applied Mechanics, vol. 61, no. 4, 2023.

[7] A. A. Cherno, "Control of Electromagnetic Vibratory Drive Using a Phase Difference Between Current Harmonics," Journal of Automation and Information Sciences, vol. 49, no. 7, 2017.

[8] A. Slabkyi "Method for parametric generation of pressure pulses by liquid and gas energy carrier with separate control of shut-off elements of a hydraulic pulse drive," Ukrainian Journal of Mechanical Engineering and Materials Science, vol. 12, no. 1, 2026.

[9] Y. Xu, Z. Wan, P. Zou, and Q. Zhang, "Experimental study on chip shape in ultrasonic vibration–assisted turning of 304 austenitic stainless steel," Advances in Mechanical Engineering, vol. 11, no. 8, 2019.

[10] D. Śniegulska-Grądzka, M. Nejman, and K. Jemielniak, "Cutting force coefficients determination using vibratory cutting," in 10th CIRP Conference on Intelligent Computation in Manufacturing Engineering, Poland, 2017

[11] J. Overcash, Tunable, ultrasonic, vibration assisted diamond turning. Charlotte, NC, USA, 2006

[12] Obertyukh, R., Slabkyi, A., Petrov, O., Bakalets, D., Sukhorukov, S. (2022). Substantiation of the Design Calculation Method for the Vibroturning Device. In: Ivanov, V., Trojanowska, J., Pavlenko, I., Rauch (eds) Advances in Design, Simulation and Manufacturing V. DSMIE 2022. Lecture Notes in Mechanical Engineering. Springer, Cham. https://doi.org/10.1007/978-3-031-06025-0_19

[13] Obertyukh R., Slabkyi A., Petrov O., and Bakalets D., "Substantiation of the methodology for calculating the design of a small-sized hydraulic pulse vibrator," Vibroengineering Procedia, Vol. 56, pp. 22–28, Oct. 2024, https://doi.org/10.21595/vp.2024.24512.

[14] Obertyukh R., Slabkyi A., Polishchuk L. K. et al.: Method of project calculation of hydroimpulsive device for vibroturning with an incorporated cycle spring pressure pulse generator. Wójcik W., Pavlov S., Kalimoldayev M. (ed.): Mechatronic Systems I. Applications in Transport, Logistics, Diagnostics and Control. Taylor & Francis Group – CRC Press, London, New York 2021, 1–16.

[15] G. E. Totten, *Handbook of Hydraulic Fluid Technology*, 2nd ed. Boca Raton, FL, USA: CRC Press, 2011.

[16] Obertyukh, R., Slabkyi, A., Povstyanoy O., Sukhorukov S; Kotyk S. (2026). Theoretical research of a new design of a parametric pressure pulse generator for a vibratory hydraulic drive.. Technologia i Automatyzacja Montażu, Vol 131 No 1 (2026). https://doi.org/10.7862/tiam.2026.1.4